THE MULTIDIMENSIONAL CONTINUOUS WAVELET TRANSFORM IN SAR IMAGING, A TOOL FOR THE OBJECT CLASSIFICATION.

M. Tria†‡ *J.P. Ovarlez*† *L. Vignaud*† *J.C. Castelli*† *and* *M. Benidir*‡

† ONERA, DEMR, BP 72, 92322 Chatillon, France

‡ L.S.S. (UMR 8506), Supelec, 3 rue Joliot Curie, 91192 Gif-sur-Yvette cedex, France

email: tria@onera.fr, ovarlez@onera.fr, vignaud@onera.fr, castelli@onera.fr, benidir@lss.supelec.fr

ABSTRACT

Usually, in radar imaging, we suppose that the reflectors respond the same way regardless of the angle from which they are viewed and have the same properties within the emitted frequency bandwidth. Nevertheless, new capacities in SAR imaging (large bandwidth, large angular excursions) make this assumption obsolete. The original application of the multidimensional continuous wavelet transform method in SAR imaging allows to highlight the frequency and angular behavior of these reflectors. This paper discusses the utility of the wavelet transform in SAR imaging for extracting from real targets some essential features allowing to distinguish objects that belong to different classes.

KEY WORDS

SAR Imaging, Wavelet Transform, Time-Frequency Distribution, Identification, Recognition, Automatic Target Recognition (ATR).

1. GENERAL DESCRIPTION OF THE PROBLEM

The radar imaging process [1, 2] consists in analyzing the backscattering coefficient $H(\vec{k})$ collected by a moving radar (see figure 1) and to form the spatial repartition $I(\vec{r})$ of the bright scatterers which reflect a part of the emitted radar signal [3, 4, 5]. The square modulus of $H(\vec{k})$ is called the Radar Cross Section (RCS) of the object for the wave vector $\vec{k}$ and is expressed in square meter. The wave vector $\vec{k}$ is related to the emitted frequency f and to the direction θ of radar illumination by relations :

$$\begin{aligned} \left|\vec{k}\right| &= \frac{2f}{c} \\ \theta &= \arg(\vec{k}) \end{aligned}$$

where c is the speed of light, and the extra-factor 2 accounts for the round trip delay (in time) of the signal.

If the object is illuminated using a broad-band signal and/or for and a large angular extent, it is realistic to consider that the amplitude of the reflectors show a dependence on frequency and on aspect angle. Such amplitude variation of scatterers has to be highlighted in order to see if this variation is potentially interpretable in terms of target characteristics.

Considering this amplitude variation, the spatial repartition of reflectors $I(\vec{r})$ must depend on the wave vector $\vec{k}$ and must now be noted $I(\vec{r},\vec{k})$.

The quantity $I(\vec{r},\vec{k})$ is, in fact, the energy distribution of the backscattering coefficient $H(\vec{k})$ in the hyperplan $(\vec{r},\vec{k})$ and will be seen, next, as ”extended images” relative to the spatial repartition $I(\vec{r})$.

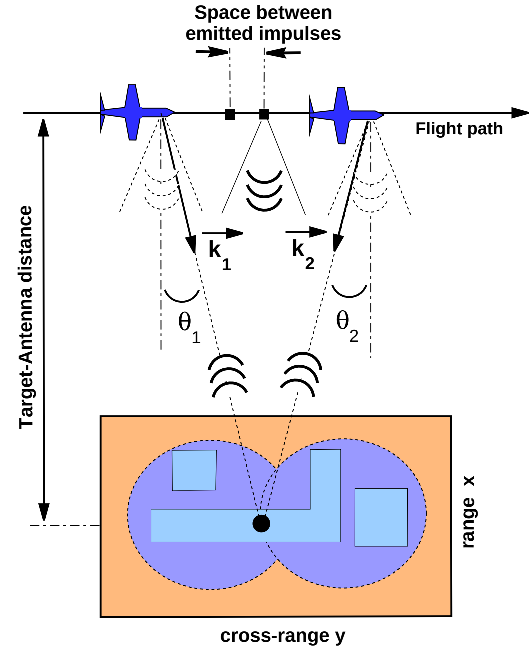

Figure 1: **A reflector, viewed at two different azimuthal angles of illumination in SAR-stripmap mode.**

2. CONSTRUCTION OF THE EXTENDED IMAGES BY WAVELET TRANSFORM

Time-frequency analysis and the physical group theory allow to construct extended radar images. These images are called hyperimages [6, 7, 8, 9, 10, 11] :

$$\tilde{I}(\vec{r}_0,\vec{k}_0) = \left| \int H(\vec{k})\, \Psi^{*}_{\vec{r}_0,\vec{k}_0}(\vec{k})\, d\vec{k} \right|^2 \tag{1}$$

where $\Psi_{\vec{r}_0,\vec{k}_0}(\vec{k})$ is a family of wavelets generated from the mother wavelet $\phi(k,\theta)$ according to :

$$\Psi_{\vec{r}_0,\vec{k}_0}(\vec{k}) \;=\; \frac{1}{k_0} e^{-2i\pi\vec{k}.\vec{r}_0}\, \phi\left(\frac{k}{k_0}, \theta-\theta_0\right). \tag{2}$$

This mother wavelet $\phi(k,\theta)$ is supposed to be localized around $(k,\theta) = (1,0)$ and positioned spatially at $\vec{r} = \vec{0}$. For example, one can use a two-dimensional separable gaussian function :

$$\phi(k,\theta) \;=\; e^{-(\frac{k-1}{\sigma_k})^2} \cdot e^{-(\frac{\theta}{\sigma_\theta})^2}$$

where the two free parameters σ_k and σ_θ control the spread in frequency and in angular domain and play on interrelated resolutions in spatial domain $\vec{r} = (x,y)$, frequency and angle.

Interpretation of the distribution $I(\vec{r},\vec{k})$

Let us rewrite $I(\vec{r},\vec{k}) \equiv I(x,y;f,\theta)$. On one hand, for each frequency f_o and each aspect angle θ_o, $I(x,y;f_o,\theta_o)$ represents a spatial repartition of reflectors which respond at this frequency and this angle. On the other hand, for each reflector located at $\vec{r_o} = (x_o,y_o)$, we can extract its energetic feature $I(x_o,y_o;f,\theta)$ as a function of frequency f and aspect angle θ. This is this aspect that we decided to point out in order to see if this quantity can be interpretable in terms of object characteristics.

To analyze this 4D structure, a visual display interface called *i4D* [12] has been developed and allows to carry out an interactive and dynamic analysis.

3. EXPERIMENTAL RESULTS OF SAR IMAGING USING WAVELETS

The first study concerns a scene composed of a building and a long metallic pipe as shown in figure 2(a) and figure 2(b). SAR imaging using wavelet analysis is illustrated in the figure 2(c) : the energy distribution in the space (f,θ) of reflectors belonging to the pipe and to the building (ridge and roof) are highlighted.

We've observed that a non-negligible number of reflectors belonging to the same object (either the pipe, or the ridge, or the roof of the building) have a similar response in frequency and aspect angle. Inversely, the response differs significatively from one structure to the other.

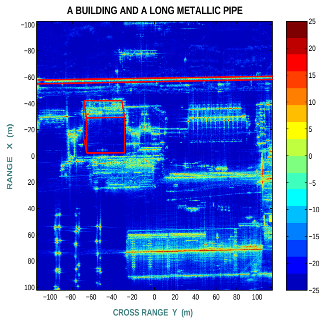

(a) SAR image of a scene including a metallic pipe and a buiding. This image has been built by RMA algorithm with data collected by the airborne radar *RAMSES* at the ONERA [13].

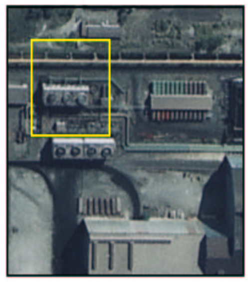

(b) Aerial photography of the scene (provided by the French National Geographic Institute). The framed portion represents the area of interest which is composed of the pipe and the building.

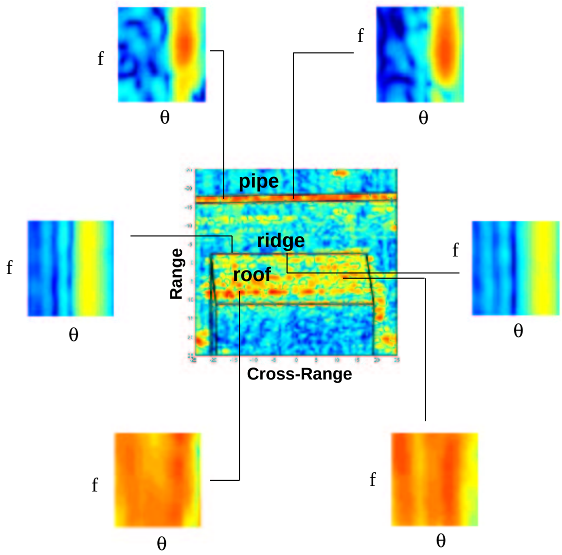

(c) **SAR imaging using wavelets : image of the building and the pipe (at the emitted frequency $f_o = 14.3$ GHz and angle illumination $\theta_o = 0.78\,°$) and energetic characteristics in the frequency-aspect angle space (f,θ) of some reflectors belonging to different structures (metallic pipe, ridge and roof of the building).**

Figure 2: **Highlighting the energetic characteristics of the image points by using wavelets in SAR imaging.**

This physical phenomenon can be explained, in part by the fact that these structures are characterized by their own geometry, material and aspect in space. Besides, a theoretical model of the energetic response of scatterers, relying on the Geometry Theory of Diffraction is proposed in the litterature [14],[15].

Then, this new kind of information can be use to separate and classify the different objects of a scene in order to make the SAR image more interpretable.

The idea that we've proposed is to compare the energetic responses of reflectors using the correlation function mentioned in the following algorithm : more the energetic responses of two reflectors are similar, stronger is the correlation of these ones.

Algorithm for object separation

Step 1 Select a point (x_o, y_o) on the image which could belong to an object.

Step 2 Determine its distribution of energy $R_{x_o,y_o}(f,\theta)$ by using the wavelet analysis. Next, this distribution will represent the reference distribution.

Step 3 Calculate the following 2D-correlation function, introducing the reference distribution and the distributions $\{R_{x_i,x_j}(f,\theta);\ (i,j) \in [1,N_x] \times [1,N_y]\ \}$ of the other points of the image :

for i:=1 to N_x

for j:=1 to N_y

$$C_o(i,j) := \frac{\int R_o(f,\theta)\ R_{i,j}(f,\theta)\ df\ d\theta}{\sqrt{E_o}\ \sqrt{E_{i,j}}}$$

end

end

where (N_x, N_y) are the numbers of points of the image respectively in range and cross-range and E is the energy associated to the response $R(f,\theta)$:

$$E \quad = \quad \int |R(f,\theta)|^2 df\ d\theta.$$

The figure 3 is the first illustration that combines the wavelet analysis and the previous algorithm for object separation. This illustration is composed of three graphics :

- On the first graphic (in the top left corner of the figure 3), we select the point of the image whose the energetic response will be taken as reference in the calculation of the 2D correlation function. This point is located on the intersection of the two red dotted line and it is supposed to belong to the object we want to separate from the rest of the image

- On the second graphic (in the bottom of the figure 3), we show the energetic distribution (calculating by wavelet analysis) of the point selected on the first graphic .

- Then, on the third one (in the top right corner of the figure 3), we point out the 2D-correlation function on the image space (x, y).

On the figure 3, a point belonging to the pipe has been selected. So the energetic distribution of this point has been took as reference in the calculation of the correlation function.

Previously, we said we've observed that many reflectors belonging to the pipe have a energetic distribution similar to the reference distribution pointed out on the second graphic of the figure 3. This observation is confirmed by the fact that the correlation is strong (more than 80 %) for most of the points on the pipe. Concerning the rest of the image, the majority of points have a distribution different from the reference distribution : the level of correlation with the reference distribution is then low. The general result is that the pipe is distinguished from the building.

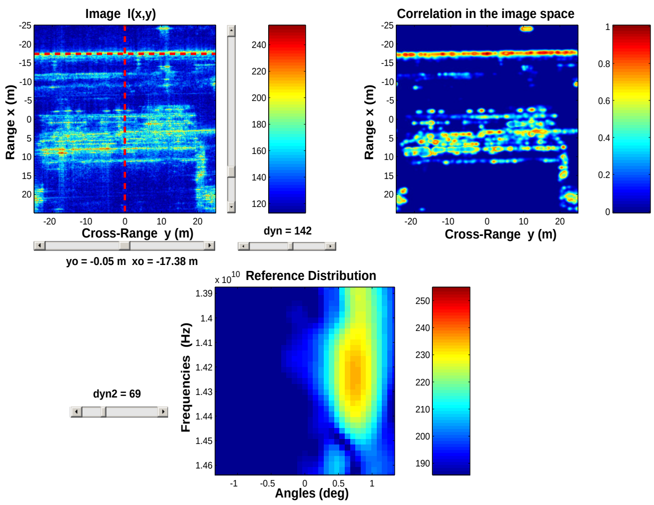

Figure 3: **Separation of the pipe from the building using the wavelet analysis combined with the correlation method.**

The second study concerns a pair of tanks with a footbridge on top of it as shows the figure 4. Between the two tanks, the footbridge extends as far as stairs on the left. The framed cell represents the area that we deal with.

First, we compute the 2D-correlation function with a reference energetic distribution corresponding to a point in the top left corner of the the tank above as shows the figure 5: the points in this part of the tank have a repartition of energy in the frequency-aspect angle space (f,θ) similar to the reference one. Moreover, some points in the same left part of the second tank below have also a distribution of energy very correlated with the reference one.

Secondly, we've selected a point on the stairs to the left of the tanks as we can see on the figure 6: the most of the reflectors that compose the stairs respond the same way with respect to the reference repartition of energy. Moreover, some points on the footbridge and on his extension on the left, have a high level of correlation with the reference distribution.

Besides, we can notice that the reference distribution, we see on the graphic in the bottom of the figure 6, means that the selected point responds the same way within the emitted frequency band but is viewed just within a very restricted aspect angle sector by the radar antenna.

To sum up this second study, we can say by comparing the two cases that the tank above can be distinguished from the stairs to the left of it.

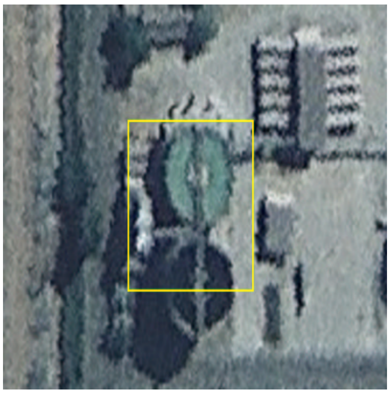

Figure 4: **Aerial photography of the area of interest including a pair of tanks and a footbridge on top with extension as far as stairs on the left.**

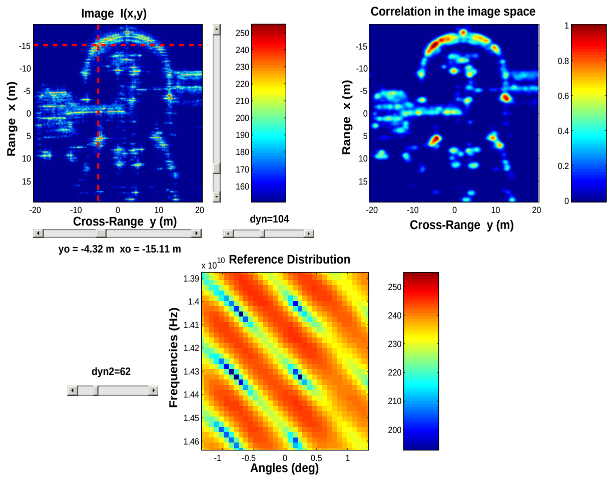

Figure 5: **A point belonging to the tank above is chosen as reference.**

The final study concerns a depot center formed by a central building and small lateral buildings (see figure 7).

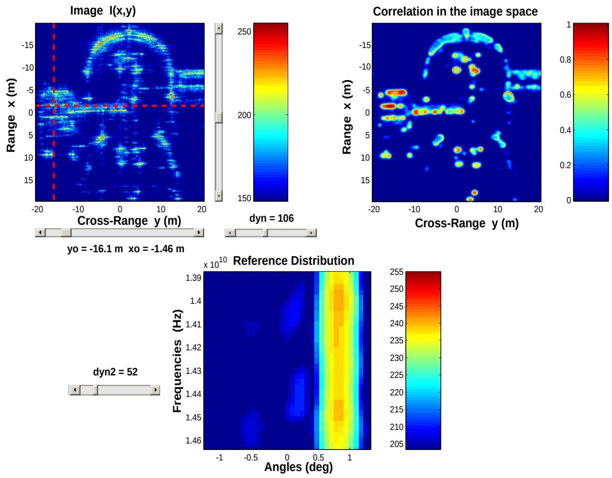

Figure 6: **A point belonging to the stairs to the left of the tanks is chosen as reference.**

Here, we select respectively a point on the top edge of the central building (see figure 8) and one point on a lateral building (see figure 9).

Clearly, by computing again the correlation function, the edge of the central building have physical characteristics that make it distinguishable from the all lateral buildings. Besides, these buildings have identical energetic features: they belongs to the same class of objects.

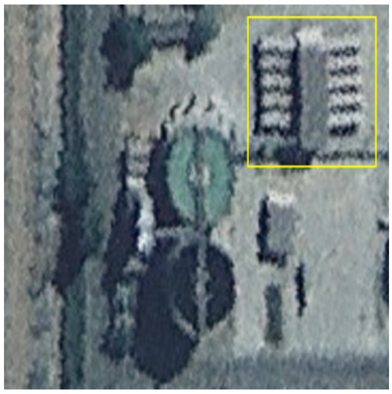

Figure 7: **Aerial photography of the scene including the depot center.**

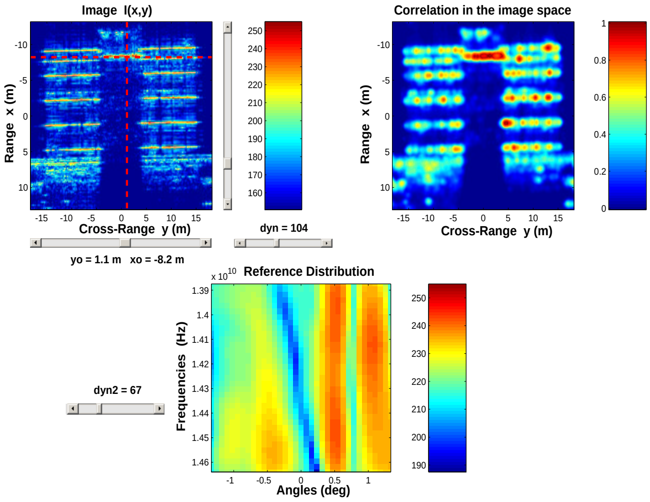

Figure 8: **A point on the top edge of the central building is chosen as reference.**

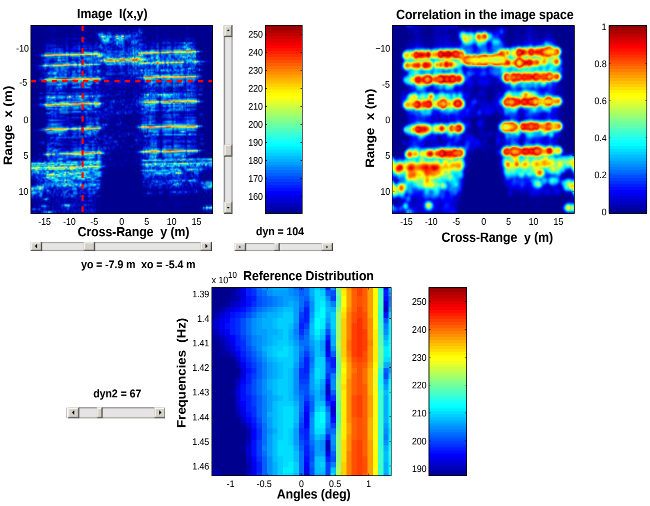

Figure 9: **A point on a lateral building is chosen as reference.**

4. CONCLUSIONS

The multidimensional wavelet transform analysis for the SAR imaging can highlight some physical characteristics of the reflectors that the classical SAR imaging can not do.

The goal was, here, to see if the energetic characteristics can be interpretable in terms of object features.

The wavelet analysis combined with the study of correlation of the energetic repartition of the reflectors show that the separation of objets is possible.

By this process, the distinction of one object from the others demands two conditions: (1) a majority of the reflectors belonging to this object must have a similar repartition of energy, defining the *energetic feature of this object*, (2) the other objects must not have a similar energetic distribution to the object's one.

Nethertheless, it can be interesting to group objects with similar energetic features within classes. It can be the case of objects with the same geometry, the same material or aspect.

To conclude, the wavelet analysis in SAR imaging with the correlation study offers a real potential for a better interpretation of the SAR images. This process can be very useful for identification and recognition of targets.

Besides, the wavelet transform method proved its usefulness, with a different approach, in polarimetry, and interferometry fields respectively by improving target identification, and providing better results on the quality of the reconstructed target height by coherence optimization [16], [17].

REFERENCES

[1] W.G. Carrara R.S. Goodman and R.M. Majewski, *Spotlight Synthetic Aperture Radar*, Artech House, Boston, London.

[2] D.L. Mensa, *High Resolution Radar Imaging*, Artech House (1981), USA.

[3] M. Soumekh, *Fourier Array Imaging*, PTR Prentice Hall (1994), Englewood Cliffs.

[4] M. Soumekh, *Synthetic Aperture Radar Signal Processing*, John Wiley & Sons, Inc.

[5] P.T. Gough D.W. Hawkins, Unified Framework for Modern Synthetic Aperture Imaging Algorithms, *Int. J. of Imaging Systems and Technology*, **8** (1997), 343-358.

[6] J. Bertrand P. Bertrand and J.P. Ovarlez, Frequency Directivity Scanning in Laboratory Radar Imaging, *Int. J. of Imaging Systems and Technology*, **5** (1994), 39-51.

[7] J.P. Ovarlez L. Vignaud J.C. Castelli M. Tria and M. Benidir, Analysis of SAR Images by Multidimensional Wavelet Transform, *IEE-Radar, Sonar and Navigation- Special Issue On Time-Frequency Analysis for Synthetic Aperture Radar and Feature Extraction*, **150**(4) (august 2003), 234-241.

[8] J.P. Ovarlez L. Vignaud J.C. Castelli M. Tria and M. Benidir, Analysis of SAR Images by Multidimensional Wavelet Transform, 5^{th} *IASTED International Conference On Signal & Image Processing*, (August 13-15, 2003), Honolulu.

[9] M. Tria, J.P. Ovarlez, L. Vignaud, J.C. Castelli and M. Benidir, SAR Imaging using Multidimensional Continuous Wavelet Transform, *to be published in Eusipco'04, XII European Signal Processing Conference* (Sept. 2004), Vienna, Austria.

[10] J. Bertrand P. Bertrand and J.P. Ovarlez, Dimensionalized Wavelet Transform with Application to Radar Imaging, *Proc. IEEE-ICASSP* (May 1991), Toronto, Canada.

[11] J. Bertrand and P. Bertrand, The Concept of Hyperimage in Wide-Band Radar Imaging, *IEEE Trans. Geosc. Remote Sensing*, **34** (1996), 1144-1150.

[12] J.C. Castelli and G. Bobillot, I4D : A New Approach to RCS Imaging Analysis, *Proc. AMTA* (Nov. 1997) Boston, USA.

[13] J.M. Boutry, ONERA Airborne SAR Facilities, *2nd International Airborne Remote Sensing Conference* (June 1996), San Francisco, USA.

[14] L.C. Potter D.M. Chiang R. Carrire and M.J. Gerry, A Geometrical Theory of Diffraction (GTD)-Based Parametric Model for Radar Scattering, *IEEE Trans. On Antennas and Propagation*, **43** (Oct. 1995), 1058-1067.

[15] L.C. Potter and R.L. Moses, Attributed Scattering Centers for SAR ATR, *IEEE Trans. On Image Processing*, **6** (Jan. 1997), 79-91.

[16] C. Titin-Schnaider, Discriminating Polarimetric Parameters for Radar Images Analysis, *Proc. IGARSS'99* (June 28-July 02, 1999), Hamburh.

[17] M. Tria and E. Colin, SAR imaging using multidimensional continuous wavelet transform and applications to polarimetry and interferometry, *Submitted to Radar2004, International Conference on Radar Systems* (Oct. 2004), Toulouse-France.